PHYSICAL REVIEW A **90**, 050501(R) (2014)

Relativistic many-body analysis of the electric dipole moment of ^{223}Rn

B. K. Sahoo,[1,*] Yashpal Singh,[1] and B. P. Das[2]

[1]*Theoretical Physics Division, Physical Research Laboratory, Navrangpura, Ahmedabad 380009, India*

[2]*Theoretical Physics and Astrophysics Group, Indian Institute of Astrophysics, Bangalore 560034, India*

(Received 12 August 2014; published 7 November 2014)

We report the results of our *ab initio* relativistic many-body calculations of the electric dipole moment (EDM) d_A arising from the electron-nucleus tensor-pseudotensor (T-PT) interaction, the interaction of the nuclear Schiff moment (NSM) with the atomic electrons and the electric dipole polarizability α_d for ^{223}Rn. Our relativistic random-phase approximation results are substantially larger than those of lower-order relativistic many-body perturbation theory and the results based on the relativistic coupled-cluster method with single and double excitations are highly accurate for all three properties that we have considered. We obtain $d_A = 4.85(6) \times 10^{-20}\langle\sigma\rangle C_T|e|$ cm from T-PT interaction, $d_A = 2.89(4) \times 10^{-17} S/(|e|\ \mathrm{fm}^3)$ from NSM interaction, and $\alpha_d = 35.27(9) e a_0^3$. The former two results in combination with the measured value of ^{223}Rn EDM, when it becomes available, could yield the best limits for the T-PT coupling constant, EDMs, and chromo-EDMs of quarks and θ_{QCD} parameter, and would thereby shed light on leptoquark and supersymmetric models that predict CP violation.

DOI: 10.1103/PhysRevA.90.050501 PACS number(s): 32.10.Dk, 11.30.Er, 24.80.+y, 31.30.jp

The observation of an electric dipole moment (EDM) of a nondegenerate system would be a signature of the violations of parity (P) and time-reversal (T) symmetries [1,2]. T violation implies charge conjugation and parity (CP) violation as a consequence of CPT invariance [3]. The standard model (SM) of elementary particle physics is able to explain the observed CP violation in the decays of neutral K [4] and B [5] mesons, but the amount of CP violation predicted by this model is not sufficient to account for the matter-antimatter asymmetry in the Universe [6,7]. The current limits for the electron EDM as well as semileptonic and hadronic CP violating coupling constants extracted by combining atomic EDM experiments and relativistic many-body calculations are several orders of magnitude higher than the predictions of these quantities by the SM [8–10]. This information cannot be obtained from the ongoing experiments at the Large Hadron Collider [11]. The study of atomic EDMs could shed light on matter-antimatter asymmetry as the origins of both these phenomena might lie beyond the SM [12].

The EDM experiments on diamagnetic and paramagnetic atoms and molecules that are currently under way could improve the sensitivity of the current measurements by a few orders of magnitudes [13–19]. The EDMs of diamagnetic atoms arise predominantly from the electron-nucleus (e-N) tensor-pseudotensor (T-PT) interaction and interaction of electrons with the nuclear Schiff moment (NSM) [20]. The e-N T-PT interaction is due to the CP violating electron-nucleon (e-n) interactions which translates to CP violating electron-quark (e-q) interactions at the level of elementary particles that are predicted by leptoquark models [20]. The NSM, on the other hand, could exist due to CP violating pion-nucleon-nucleon (π-n-n) interactions and the EDM of nucleons and both of them in turn could originate from CP violating quark-quark (q-q) interactions or EDMs and chromo-EDMs of quarks that are predicted by certain supersymmetric models [8–10]. In order to obtain precise limits for the coupling constants of these interactions and EDMs of quarks, it is necessary to perform both experiments and calculations as accurately as possible on suitable atoms.

According to the Schiff theorem [21], the EDM of a system vanishes if it is treated as pointlike and in the nonrelativistic approximation even if its constituents have nonzero EDMs. However, if relativistic and finite-size effects are taken into account, then they not only give rise to a nonzero EDM of a composite system, but also play an important role in enhancing it [22]. The EDM of a composite system could be larger than those of its individual constituents due to their coherent contributions and, also, the internal structure of these systems in some cases can further enhance these effects overwhelmingly; owing to which observations of EDMs in these systems might be possible. In general, heavy atomic systems are best suited for EDM measurements. A case in point is the diamagnetic ^{223}Rn atom, which is sensitive to the T-PT and NSM interactions.

The e-n T-PT interaction Hamiltonian is given by [20,23]

$$H^{e\text{-}n}_{\text{T-PT}} = \frac{G_F}{\sqrt{2}} C_T^{e\text{-}n} \bar{\psi}_e \gamma_5 \sigma_{\mu\nu} \psi_e \bar{\psi}_n \iota \gamma_5 \sigma_{\mu\nu} \psi_n, \tag{1}$$

where $C_T^{e\text{-}n}$ is the dimensionless e-n T-PT interaction coupling coefficient, $\sigma_{\mu\nu} = (\gamma_\mu\gamma_\nu - \gamma_\nu\gamma_\mu)/2$ where the γ's are the usual Dirac γ matrices and G_F is the Fermi constant. This corresponds to the e-N T-PT interaction Hamiltonian (H_{int}) in an atom as

$$H_{\text{int}} \equiv H^{\text{T-PT}}_{\text{EDM}} = i\sqrt{2} G_F C_T \sum_e \boldsymbol{\sigma_N} \cdot \boldsymbol{\gamma_e} \rho_N(r_e), \tag{2}$$

where C_T is the e-N T-PT coupling constant, $\boldsymbol{\sigma}_N = \langle\sigma_N\rangle \frac{\mathbf{I}}{I}$ is the Pauli spinor of the nucleus for the nuclear spin I, $\rho_N(r)$ is the nuclear density, and subscript e represents the electronic coordinate.

The e-N NSM interaction Hamiltonian is given by [24]

$$H_{\text{int}} \equiv H^{\text{NSM}}_{\text{EDM}} = \frac{3\mathbf{S}\cdot\mathbf{r}}{B_4} \rho_N(r), \tag{3}$$

*bijaya@prl.res.in

where $\mathbf{S} = S\frac{\mathbf{I}}{I}$ is the NSM and $B_4 = \int_0^\infty dr\, r^4 \rho_N(r)$. The magnitude of NSM S is given by [25–27]

$$S = g_{\pi nn}\left(a_0 \bar{g}^{(0)}_{\pi nn} + a_1 \bar{g}^{(1)}_{\pi nn} + a_2 \bar{g}^{(2)}_{\pi nn}\right), \tag{4}$$

where $g_{\pi nn} \simeq 13.5$ is the CP-even π-n-n coupling constant, a_i's are the polarizations of the nuclear charge distribution that can be computed to reasonabe accuracy using the Skyrme effective interactions or the Hartree-Fock-Bogoliubov mean-field method [25–27], and $\bar{g}^{(i)}_{\pi nn}$'s with $i = 1,2,3$ represent the isospin components of the CP-odd π-n-n coupling constants. Owing to the extremely small value of $\bar{g}^{(2)}_{\pi nn}$, it is generally neglected in the literature while imposing upper limits on $\bar{g}^{(0)}_{\pi nn}$ and $\bar{g}^{(1)}_{\pi nn}$. They are related to the up- and down-quark chromo-EDMs $\tilde{d}_u$ and $\tilde{d}_d$ as $\bar{g}^{(1)}_{\pi nn} \approx 2 \times 10^{-12}(\tilde{d}_u - \tilde{d}_d)$ [28] and $\bar{g}^{(0)}_{\pi nn}/\bar{g}^{(1)}_{\pi nn} \approx 0.2(\tilde{d}_u + \tilde{d}_d)/(\tilde{d}_u - \tilde{d}_d)$ [29].

To date the best limit for the EDM of a diamagnetic atom (d_A) is obtained from ^{199}Hg as $d_A < 3.1 \times 10^{-29}|e|$ cm [30]. The EDM of ^{223}Rn has been estimated to be a factor of 400 to 600 times larger than that of ^{199}Hg [31]. This enhancement together with a sensitivity of $10^{-26}|e|$ cm to $10^{-27}|e|$ cm that has been projected for an experiment on this isotope of Rn [32,33] could yield a better limit for d_A relative to ^{199}Hg EDM [30]. Moreover, the values of a_i determined using different Skyrme interactions vary over a wide range in Hg and in some cases, even their signs are opposite [26,27]. It is therefore problematic to infer limits on quark chromo-EDMs reliably. In contrast, these quantities can be evaluated quite consistently for Rn with various Skyrme interactions [26], making it a more suitable candidate for EDM studies than Hg. It is necessary to improve the calculations of d_A/C_T and d_A/S for ^{223}Rn so that when the EDM measurement is available, we can combine the two results to get more accurate limits for C_T and S than those that are currently available. The earlier calculations of d_A/C_T and d_A/S for ^{223}Rn were performed in [34,35] using the relativistic random-phase approximation (RPA) to account for the correlation effects. Recently, we have developed and employed the Dirac-Fock (DF) method, second- [MBPT(2)] and third- [MBPT(3)] order many-body perturbation theory (MBPT), RPA, and coupled-cluster (CC) methods in the four-component relativistic framework for the closed-shell atomic systems from different groups of the periodic table to study the passage of the correlation effects from one level of approximation to another in the calculations of the ground state electric dipole polarizabilities (α_d) [36,37] and ^{129}Xe EDM [38]. Given that the rank and parity of the dipole operator are the same as those of the electronic component of the T-PT and NSM interaction Hamiltonians, some insights into the accuracies of d_A calculations for the closed-shell atoms can be provided by the calculations of α_d by considering $H_{\rm int}$ as the electric dipole operator D. No measurement for α_d of a Rn atom has been reported so far and all the previous calculations of this quantity are not in good agreement with each other [39–43]. In this Rapid Communication, we use the aforementioned methods to determine α_d and the EDM of a ^{223}Rn atom from the T-PT interaction and NSM with the purpose of elucidating the role of the correlation effects in different many-body approximations.

We consider the DF wave function $|\Phi_0\rangle$ as the starting point and electron correlation effects are incorporated at different levels of approximation through the relativistic MBPT(2), MBPT(3), RPA, and CC methods. In our relativistic CC calculations, we have considered the single and double excitations retaining only the linear terms (LCCSD method) as well as all the linear and nonlinear terms (CCSD method). In both cases, we consider the Dirac-Coulomb (DC) Hamiltonian which is given in atomic units (a.u.) by

$$H = \sum_i \left[c\boldsymbol{\alpha}_i \cdot \mathbf{p}_i + (\beta_i - 1)c^2 + V_N(r_i) + \sum_{j>i} \frac{1}{r_{ij}} \right], \tag{5}$$

where $\boldsymbol{\alpha}_i$ and β_i are the Dirac matrices, $V_N(r)$ is the nuclear potential obtained using the Fermi charge distribution, and r_{ij}'s are the interelectronic distances.

In the presence of $H_{\rm int}$, the ground state wave function of an atom can be approximated to

$$|\Psi_0\rangle \simeq \left|\Psi_0^{(0)}\right\rangle + \lambda\left|\Psi_0^{(1)}\right\rangle, \tag{6}$$

where $|\Psi_0^{(0)}\rangle$ and $|\Psi_0^{(1)}\rangle$ are the unperturbed wave functions corresponding to the DC Hamiltonian and its first-order correction due to $H_{\rm int}$, represented by a parameter λ, respectively. In the CC method, we express

$$\begin{aligned} |\Psi_0\rangle &= e^T|\Phi_0\rangle = e^{T^{(0)}+\lambda T^{(1)}}|\Phi_0\rangle \\ &\simeq e^{T^{(0)}}(1+\lambda T^{(1)})|\Phi_0\rangle, \end{aligned} \tag{7}$$

with the CC operators $T^{(0)}$ and $T^{(1)}$ creating even and odd parity excitations, respectively, from $|\Phi_0\rangle$ due to the electron correlation effects. It therefore follows that

$$\left|\Psi_0^{(0)}\right\rangle = e^{T^{(0)}}|\Phi_0\rangle \quad \text{and} \quad \left|\Psi_0^{(1)}\right\rangle = e^{T^{(0)}}T^{(1)}|\Phi_0\rangle. \tag{8}$$

The solution for $|\Psi_0^{(1)}\rangle$ is obtained by solving an equation equivalent to the first-order perturbed equation given by

$$(H - E^{(0)})\left|\Psi_0^{(1)}\right\rangle = (E^{(1)} - H_{\rm int})\left|\Psi_0^{(0)}\right\rangle, \tag{9}$$

where $E^{(0)}$ is the eigenvalue energy of $|\Psi_0^{(0)}\rangle$ and $E^{(1)}$ is its first-order correction due to $H_{\rm int}$ which vanishes in the present case. In the LCCSD and CCSD methods, the single and double excitations are denoted with the subscripts 1 and 2 of T operators, respectively.

The final expression used to evaluate α_d and EDMs (commonly referred to as X) is given by

$$\begin{aligned} X &= \frac{\langle\Psi_0|D|\Psi_0\rangle}{\langle\Psi_0|\Psi_0\rangle} = \frac{\langle\Phi_0|e^{T^\dagger}De^T|\Phi_0\rangle}{\langle\Phi_0|e^{T^\dagger}e^T|\Phi_0\rangle} \\ &\simeq 2\frac{\langle\Phi_0|\,\widetilde{D^{(0)}}\,T^{(1)}|\Phi_0\rangle}{\langle\Phi_0|e^{T^{\dagger(0)}}e^{T^{(0)}}|\Phi_0\rangle} = 2\langle\Phi_0|(\widetilde{D^{(0)}}\,T^{(1)})_c|\Phi_0\rangle, \end{aligned} \tag{10}$$

with $\widetilde{D^{(0)}} = e^{T^{\dagger(0)}}De^{T^{(0)}}$, which in the LCCSD method terminates to $\widetilde{D^{(0)}} = D + DT^{(0)} + T^{\dagger(0)}D + T^{\dagger(0)}DT^{(0)}$ and the subscript c means the terms are connected.

We present the results of α_d and d_A of our calculations and those of other calculations in Table I. Among these results, we consider the CCSD results to be the most accurate on physical grounds. We first discuss our α_d results for the ground state of Rn. There is no experimental result available for this quantity.

TABLE I. Results of α_d in ea_0^3, d_A due to T-PT interaction (d_A^T) in $\times 10^{-20}\langle\sigma\rangle C_T|e|$ cm and d_A due to NSM (d_A^S) in $\times 10^{-17} S/(|e|\ \mathrm{fm}^3)$ of the ground state of ^{223}Rn using different many-body methods. "Others" refers to previous results from other works.

Employed	This work			Others		
method	α_d	d_A^T	d_A^S	α_d	d_A^T	d_A^S
DF	34.42	4.485	2.459	34.42[a], 33.54[b]		2.47[a]
				29.22[c], 32.81[d]	4.6[e,f]	2.5[e,f]
MBPT(2)	29.57	3.927	2.356	28.48[c], 33.19[d]		
				32.6[g]		
MBPT(3)	18.10	4.137	2.398			
RPA	35.00	5.400	3.311	35.00[a], 32.75[b]		3.33[a]
					5.6[e,f]	3.3[e,f]
LCCSD	35.08	5.069	3.055			
CCSD	35.27(9)	4.85(6)	2.89(4)	34.39[b], 28.61[c]		
				32.90[d], 35.391[h]		
			Error budget			
Triples	0.01	− 0.003	− 0.005			
QED[i]	0.02	0.053	0.028			
Breit[i]	0.09	− 0.020	− 0.033			

[a]Reference [34].
[b]Results are quoted from basis 2 of [39].
[c]Reference [40].
[d]Reference [42].
[e]Calculations are for ^{211}Rn.
[f]Reference [35].
[g]Reference [41].
[h]Reference [43].
[i]Calculations are estimated using RPA.

Broadly, the approaches followed in the calculations of α_d can be classified into two categories. The results reported in [39–42] are obtained by evaluating the second derivative of the ground state energy with respect to an arbitrary electric field. However, the calculations carried out in [34,43] and by us involve the determination of the expectation value of D in the ground state which has a mixed parity wave function due to $H_{\rm int} \equiv D$. Our results at the DF and RPA levels agree very well with those of Ref. [34]. The agreement between the results of our CCSD and another similar work, Ref. [43], is also very good. Our T-PT and NSM EDM results for ^{223}Rn at the DF and RPA levels agree with those of Refs. [34,35]. Our EDM results using the CCSD method which subsumes the DF, RPA, and all-order non-RPA (the rest apart from RPA) contributions are clearly the most rigorous to date.

We also estimate uncertainties to our CCSD results by determining contributions from important triple excitations by defining a perturbative triple excitation operator (CCSD$_p T$ method), as described in [37,38], and using it in Eq. (10), from the frequency independent Breit interaction given by

$$V_B(r_{ij}) = -\frac{1}{2r_{ij}}\{\boldsymbol{\alpha}_i\cdot\boldsymbol{\alpha}_j + (\boldsymbol{\alpha}_i\cdot\hat{\mathbf{r}}_{\mathbf{ij}})(\boldsymbol{\alpha}_j\cdot\hat{\mathbf{r}}_{\mathbf{ij}})\} \tag{11}$$

and from the lower-order vacuum polarization effects from the quantum electrodynamics (QED) corrections through the Uehling [$V_U(r)$] and Wichmann-Kroll [$V_{\rm WK}(r)$] potentials given by

$$V_U(r) = -\frac{4}{9c\pi}V_N(r)\int_1^\infty dt\sqrt{t^2-1}\left(\frac{1}{t^2}+\frac{1}{2t^4}\right)e^{-2ctr} \tag{12}$$

and

$$V_{\rm WK}(r) = -\frac{2}{3}\frac{1}{c\pi}V_N(r)\frac{0.092c^2Z^2}{1+(1.62cr)^4} \tag{13}$$

with Z as the atomic number of the atom. Contributions from the Breit and QED interactions are estimated using RPA and they are given in Table I towards the bottom under error budget. Although these contributions for EDMs cancel out, we have added them using the quadrature formula to find out the net uncertainties of all the quantities that are given in the parentheses alongside the CCSD results.

It can be seen from Table I that the correlation trends for α_d and d_A are different. A possible reason for this is that even though all the $H_{\rm int}$ operators that have been considered have the same rank and parity, only the $s_{1/2}$ and $p_{1/2}$ orbitals contribute predominantly to d_A, while other higher symmetry orbitals also contribute significantly in the case of α_d. The trends for both the T-PT and NSM interactions seem to be qualitatively similar, but the relative sizes of the correlation contributions are different for the two cases.

The following conclusions can be drawn from Table I: (i) The lower-order RPA effects are appreciable in magnitude and they reduce the MBPT(2) and MBPT(3) results relative to that of the DF values. Their higher-order counterparts are collectively large and this is reflected in the final RPA results for our α_d and EDM calculations. (ii) There are significant cancellations between the all-order RPA and the all-order non-RPA contributions at the CCSD level for the EDMs. The inclusion of the non-RPA terms which first appear in MBPT(3) in a perturbative theory framework, is therefore crucial. (iii) There are cancellations between the linear and nonlinear CCSD terms for the EDMs. It is therefore imperative to use an all-order approach like the CCSD method to capture the above-mentioned points. In order to identify which non-RPA diagrams take part in the cancellations, we give a few of these diagrams in Fig. 1 at the MBPT(3) level and their contributions explicitly in Table II.

The differences in the LCCSD and CCSD results given in Table I highlight the importance of the nonlinear correlation terms such as $T_1^{(0)}T_2^{(0)}, \frac{1}{2}T_2^{(0)}T_2^{(0)}, \ldots$, which correspond to the contributions from higher level excitations such as triples,

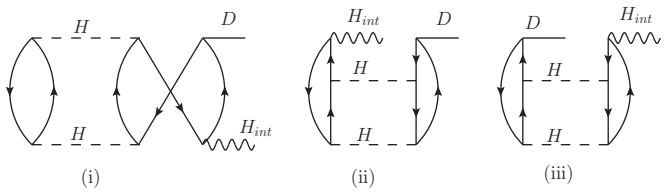

FIG. 1. A few important non-RPA diagrams from the MBPT(3) method. Here (ii) is obtained by contracting $H_{\rm int}$ with the second-order unperturbed wave operator, while (iii) is from the contraction of a Coulomb operator with the first-order perturbed wave operator. Lines with up and down arrows represent occupied and unoccupied orbitals, respectively.

TABLE II. Individual contributions from the non-RPA diagrams that are shown in Fig. 1.

Diagram	α_d	d_A^T	d_A^S
(i)	−4.522	−0.339	−0.241
(ii)	−1.166	−0.086	−0.051
(iii)	−1.137	−0.053	−0.039

quadruples, etc. A detailed analysis of our calculations reveals that the role of the nonlinear effects is more significant when included in the wave functions rather than in the exponential terms in Eq. (10). This can be observed from the contributions of the linear CC terms in the LCCSD and CCSD methods in Table III. Results given as "Others" from the CCSD method are the nonlinear contributions from the exponential terms in the expectation value given in Eq. (10).

In conclusion, we give the results of our CCSD calculations as our recommended values for ^{223}Rn EDMs, i.e., $d_A = 4.853 \times 10^{-20}\langle\sigma\rangle C_T|e|$ cm and $d_A = 2.892 \times 10^{-17} S/(|e|\ \text{fm}^3)$. They are both about nine times larger than the results for ^{129}Xe that we had reported recently [38]. Our Schiff moment calculation could be combined with the future measured value of ^{223}Rn EDM to give limits for the EDMs and chromo-EDMs of quarks and the θ_{QCD} parameter that would be competitive with those obtained from a few other heavy closed-shell atoms. These limits have the potential to provide a wealth of information on new physics beyond the SM. Our ground state polarizability result of the Rn atom will be useful in the context of the EDM studies of ^{223}Rn and its experimental verification.

TABLE III. Contributions from CC terms to α_d and d_A (with the same units as in Table I) from the LCCSD and CCSD methods.

CC	LCCSD			CCSD		
terms	α_d	d_A^T	d_A^S	α_d	d_A^T	d_A^S
$DT_1^{(1)}$	37.747	4.881	2.960	37.492	4.630	2.774
$T_1^{(0)}\ DT_1^{(1)}$	−0.166	0.015	0.007	−0.319	0.005	-3×10^{-4}
$T_2^{(0)}\ DT_1^{(1)}$	−3.827	0.248	0.099	−4.166	0.308	0.132
$T_1^{(0)}\ DT_2^{(1)}$	−0.052	0.004	0.002	−0.074	0.002	0.001
$T_2^{(0)}\ DT_2^{(1)}$	1.380	−0.079	−0.013	1.400	−0.087	−0.014
Others				−0.093	−0.005	−0.001

[1] L. Landau, Nucl. Phys. **3**, 127 (1957).
[2] N. F. Ramsey, Phys. Rev. **109**, 225 (1958).
[3] G. Luders, Ann. Phys. (NY) **281**, 1004 (2000).
[4] J. H. Christenson, J. W. Cronin, V. L. Fitch, and R. Turlay, Phys. Rev. Lett. **13**, 138 (1964).
[5] R. Aaij *et al.* (LHCb Collaboration), Phys. Rev. Lett. **110**, 221601 (2013).
[6] L. Canetti, M. Drewes, and M. Shaposhnikov, New J. Phys. **14**, 095012 (2012).
[7] M. Dine and A. Kusenko, Rev. Mod. Phys. **76**, 1 (2003).
[8] M. Pospelov and A. Ritz, Ann. Phys. (NY) **318**, 119 (2005).
[9] S. M. Barr, Int. J. Mod. Phys. A **8**, 209 (1993).
[10] T. Fukuyama, Int. J. Mod. Phys. A **27**, 1230015 (2012).
[11] N. Fortson, P. Sandars, and S. Barr, Phys. Today **56**(6), 33 (2003).
[12] A. M. Kazarian, S. V. Kuzmin, and M. E. Shaposhnikov, Phys. Lett. B **276**, 131 (1992).
[13] T. Furukawa, T. Inoue, T. Nanao, A. Yoshimi, M. Tsuchiya, H. Hayashi, M. Uchida, and K. Asahi, J. Phys.: Conf. Ser. **312**, 102005 (2011).
[14] T. Inoue *et al.*, Hyperfine Interact. **220**, 59 (2013).
[15] D. S. Weiss (private communication).
[16] D. Heinzen (private communication).
[17] Y. Sakemi *et al.*, J. Phys.: Conf. Ser. **302**, 012051 (2011).
[18] J. Baron *et al.* (The ACME Collaboration), Science **343**, 269 (2014).
[19] J. J. Hudson, D. M. Kara, I. J. Smallman, B. E. Sauer, M. R. Tarbutt, and E. A. Hinds, Nature (London) **473**, 493 (2011).
[20] S. M. Barr, Phys. Rev. D **45**, 4148 (1992).
[21] L. I. Schiff, Phys. Rev. **132**, 2194 (1963).
[22] P. G. H. Sandars, Phys. Lett. **14**, 194 (1965).
[23] A.-M. Maartensson-Pendrill, Phys. Rev. Lett. **54**, 1153 (1985).
[24] V. V. Flambaum and J. S. M. Ginges, Phys. Rev. A **65**, 032113 (2002).
[25] W. C. Haxton and E. M. Henley, Phys. Rev. Lett. **51**, 1937 (1983).
[26] S. Ban, J. Dobaczewski, J. Engel, and A. Shukla, Phys. Rev. C **82**, 015501 (2010).
[27] J. H. de Jesus and J. Engel, Phys. Rev. C **72**, 045503 (2005).
[28] M. Pospelov, Phys. Lett. B **530**, 123 (2002).
[29] W. Dekens, J. de Vries, J. Bsaisou, W. Bernreuther, C. Hanhart, Ulf-G. Meissner, A. Nogga, and A. Wirzba, J. High Energy Phys. **1407**, 069 (2014).
[30] W. C. Griffith M. D. Swallows, T. H. Loftus, M. V. Romalis, B. R. Heckel, and E. N. Fortson, Phys. Rev. Lett. **102**, 101601 (2009).
[31] N. Auerbach, V. V. Flambaum, and V. Spevak, Phys. Rev. Lett. **76**, 4316 (1996).
[32] E. T. Rand *et al.*, J. Phys.: Conf. Ser. **312**, 102013 (2011).
[33] Tardiff *et al.*, Hyperfine Interact. **225**, 197 (2014).
[34] V. A. Dzuba, V. V. Flambaum, J. S. M. Ginges, and M. G. Kozlov, Phys. Rev. A **66**, 012111 (2002).
[35] V. A. Dzuba, V. V. Flambaum, and S. G. Porsev, Phys. Rev. A **80**, 032120 (2009).
[36] Y. Singh, B. K. Sahoo, and B. P. Das, Phys. Rev. A **88**, 062504 (2013).
[37] Y. Singh and B. K. Sahoo, Phys. Rev. A **90**, 022511 (2014).
[38] Y. Singh, B. K. Sahoo, and B. P. Das, Phys. Rev. A **89**, 030502(R) (2014).
[39] N. Runeberg and P. Pyykkö, Int. J. Quantum Chem. **66**, 131 (1998).
[40] C. S. Nash, J. Phys. Chem. A **109**, 3493 (2005).
[41] B. O. Roos, R. Lindh, P.-A. Malmqvist, V. Beryazov, and P.-O. Widmark, J. Phys. Chem. **108**, 2851 (2004).
[42] T. Nakajima and K. Hirao, Chem. Lett. **30**, 766 (2001).
[43] S. Chattopadhyay, B. K. Mani, and D. Angom, Phys. Rev. A **86**, 062508 (2012).